

Variable-Decision Frequency Option Critic

Amirmohammad Karimi^{1,†}, Jun Jin³, Jun Luo³, A. Rupam Mahmood^{1,4}, Martin Jagersand¹, Samuele Tosatto²

Abstract—In classic reinforcement learning algorithms, agents make decisions at discrete and fixed time intervals. The physical duration between one decision and the next becomes a critical hyperparameter. When this duration is too short, the agent needs to make many decisions to achieve its goal, aggravating the problem’s difficulty. But when this duration is too long, the agent becomes incapable of controlling the system. Physical systems, however, do not need a constant control frequency. For learning agents, it is desirable to operate with low frequency when possible and high frequency when necessary. We propose a framework called Continuous-Time Continuous-Options (CTCO), where the agent chooses options as sub-policies of variable durations. Such options are time-continuous and can interact with the system at any desired frequency providing a smooth change of actions. The empirical analysis shows that our algorithm is competitive w.r.t. other time-abstraction techniques, such as classic option learning and action repetition, and practically overcomes the difficult choice of the decision frequency.

I. INTRODUCTION

Perception, decisions, and actions are the three building blocks of autonomous systems [1]. Perception consists of sensing the surrounding environment using camera, force and tactile sensors, lidars, and many others. Acting allows the agent to change the state of the environment. Robotic agents typically alter their own configuration (i.e., their position in space) to interact with the environment. Decision connects perception and actions: the role of a learning agent is to discover the optimal mapping between perceptions to actions to achieve a specific goal.

Actions can have different levels of abstraction. Low-level actions (e.g., joint positions, velocities, or torques) are flexible as they express a rich set of behaviors but typically require high-frequency decision-making [2], thereby complicating learning and inducing sample inefficiency. High-level actions are often preferable as they require lower decision frequency, making learning more straightforward and efficient. However, they are task-specific, require human knowledge, and can hinder optimal behavior [3], [4]. The choice of the action space impacts the performance of the learning agent, introducing a complex dilemma: *which action space and decision frequency should be the best one?*

High-level actions are still composed of low-level actions. For example, a grasping movement primitive still expresses

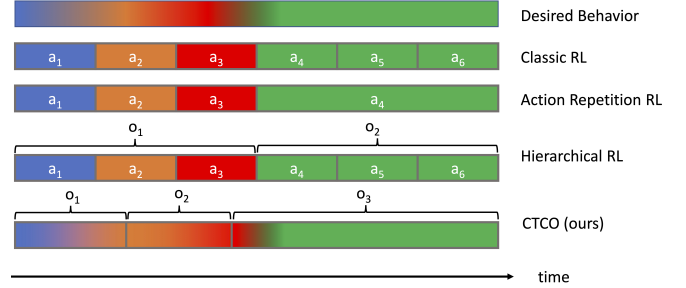


Fig. 1: A graphic visualization of different discretization techniques. The horizontal bars depict the change in time (from left to right) of action (represented with color). The desired behavior changes smoothly in time. Classic RL applies a uniform discretization, and action durations must be chosen in advance. ARRL implements temporal abstractions by repeating the same actions multiple times. HRL uses options that, similarly to classic RL, use discrete-time actions. Our framework CTCO has options with variable durations chosen by the agent.

a (long) sequence of low-level actions (e.g., joint or torques). Designing learning agents is more convenient when movement primitives are used instead of torques because they provide a higher level of abstraction [5]. With movement primitives, the learner can observe the environment less frequently and make fewer decisions to reach its goal.

Hierarchical RL (HRL) aims to provide a higher level of abstraction without losing flexibility [6]. In HRL, the policy selects lower-level policies called *options* [7], [8]. From the policy perspective, options are high-level actions and can be chosen with low frequency. The set of options is finite, and options must be learned and adapted to the task. However, learning options is difficult as they are defined with low-level action space and require fixed high decision frequency. HRL helps provide more efficient learning, but the options’ high decision frequency remains a bottleneck. Furthermore, learning policy and options simultaneously is often challenging due to the high redundancy of possible solutions.

In this paper, we argue that the decision frequency does not necessarily need to be fixed. Typically, the decision frequency should be higher when the system is hard to control [2], while it can be lower otherwise. A good example is the swing-up pendulum task. During the “swinging phase”, the system is simple to control, and one can decide to swing left or right with low frequency until the pendulum

¹ Department of Computer Science, University of Alberta, Edmonton, Canada. ² Department of Computer Science and Digital Science Center, University of Innsbruck, Innsbruck, Austria.

³Noah’s Ark Lab, Huawei Technologies Canada, Edmonton, Canada.

⁴Alberta Machine Intelligence Institute (Amii)

[†] Corresponding author: amirmoha@ualberta.ca

is upright. In the stabilization phase, however, the system is unstable, and one needs to apply frequent small torques in different directions to compensate for perturbations. In other words, one can make the learning algorithm more efficient by allowing the agent to make decisions less frequently when possible.

Action-repetition RL (ARRL) introduces a temporal abstraction method by repeating actions for a variable number of steps [9], [10]. This dynamic repetition has the effect of providing a variable decision frequency. In ARRL, the action space is augmented with a set of discrete numerical values describing the number of steps for which action should be repeated, allowing making decisions with lower frequency when needed, consequently increasing learning efficiency. ARRL is conceptually simpler than HRL, suffers less redundancy, and does not require learning options. However, its simplicity has a substantial downside: repeating the same action for a long time is rarely a satisfying solution to real-world problems and, the policy cannot fully exploit temporal abstraction.

Continuous-time RL (CTRL) mitigates learning problems related to high frequencies as policies are continuous-time [11]. Continuous-time RL abstracts from the actual hardware implementation, which typically works in discrete time, allowing the impact of the controlling frequency on the learning system altogether. Unfortunately, CTRL is much more complicated than classic RL ([12], [13]). For this reason, it is rarely used in real-world problems.

Time-correlated exploration. Deep deterministic policy gradient (DDPG) [14] was among the first off-policy algorithm to propose temporally correlated noise to provide better exploration. The idea of temporally or non-Markov exploration has been further investigated in the literature, e.g., [15]. Recently, Mutti et al., 2021 [16] proposed that the optimal exploration policy can be *deterministic* but non-Markovian. In summary, exploring with some sort of explicit time-dependency or following a non-Markovian mechanism has been shown to be beneficial for the learning system.

Contributions. In this paper, we developed Continuous-Time Continuous-Options (CTCO) framework that can be seen as halfway between full HRL and ARRL and is defined in continuous time to allow scalability with high frequencies. Like HRL [6], our system has a policy that selects options. However, unlike classic HRL [7], [8], [6], our approach considers an infinite set of options, overcoming the need to learn them. Learning options was necessary for HRL because the set of options was finite; therefore, each option needed to be adapted to the task. However, when the set of options is comprehensive enough, there is no need to revise them. Similar to ARRL [9], [10], the space of options is augmented with continuous values defining option durations, but our options are more expressive than a constant action repetition. Figure 1 illustrates these differences. Continuous durations are independent of the effective action frequency (e.g., the controller frequency), making our learning system robust w.r.t. high-frequencies. In our experiments, we show that: 1) differently from classic RL, HRL, and ARRL, our

algorithm is robust w.r.t. high action frequencies and 2) the correlated exploration of our time-dependent options helps in sparse reward tasks. Our experiments are conducted on four classic RL benchmarks from MuJoCo and OpenAI, as well as on a 7 DoF real robotic manipulator.

II. BACKGROUND

Discrete-Time Decision-Making is formalized using Markov decision processes (MDPs) $\langle \mathcal{S}, \mathcal{A}, p, r, \gamma, \mu_0 \rangle$, where \mathcal{S} is the set of states; \mathcal{A} is the set of actions; $p(s'|s, a)$ is the probability of visiting $s' \in \mathcal{S}$ after the application of action $a \in \mathcal{A}$ to state $s \in \mathcal{S}$; $r(s, a)$ is the reward signal in state s and action a , γ is the discount factor and μ_0 is the distribution of starting states. *Decisions* are often encoded with a stochastic parametric model $a \sim \pi_\theta(s)$ where θ is the set of parameters. The goal of reinforcement learning is to find the set of parameters that maximizes the discounted objective

$$J_\pi^\gamma(\theta) := \mathbb{E}_\pi \left[\sum_{t=0}^{\infty} \gamma^t r(s_t, a_t) \right]. \quad (1)$$

In discrete time decision-making, there is no notion of physical time: the time elapsed between two consecutive state observations is not considered. However, when implemented on the real system, the designer needs to decide *when* the system needs to observe the environment and make decisions. Since the physical time is not considered in this mathematical mode, the time interleaving two observations (or decisions) is usually kept constant. The time interleaving two consecutive decisions determines the learning agent's frequency, and it heavily impacts the performances [17].

Continuous-Time Decision-Making assumes a continuous evolution of states, actions, and rewards defined with a *time-independent* dynamical system [11]

$$\dot{s}_t = f(s_t, a_t). \quad (2)$$

For simplicity, Equation 2 does not consider stochasticity, which can be formalized with a more rigorous set of assumptions. Informally, such assumptions ensure that the probability of observing a state s_t after a continuous sequence of actions $a_{0:t}$ starting from a given state s_t is Markovian, i.e.,

$$p(s_{t+d}|s_t, a_{t:t+d}) = p(s_{t+d}|s_t, a_{0:t+d}). \quad (3)$$

where $d > 0$ denotes the duration of the sequence. Furthermore, the system is time-invariant, i.e.,

$$p(s_{t_1+d}|s_{t_1}, a_{t_1:t_1+d}) = p(s_{t_2+d}|s_{t_2}, a_{t_2:t_2+d}) \quad (4)$$

$$\forall t_1, t_2 \geq 0 \text{ s.t. } s_{t_1} = s_{t_2}, a_{t_1:t_1+d} = a_{t_2:t_2+d} \quad (5)$$

In infinite-horizon problems, the discounted objective becomes

$$J_\pi^r(a_{0:\infty}) = \mathbb{E} \left[\int_0^{\infty} e^{-\tau t} r(s_t, a_t) dt \right]. \quad (6)$$

A Unified View. The continuous system described can be viewed as a discrete system too [18]. This second view is

more convenient because it allows using existing tools for discrete processes to optimize the continuous systems. Consider the following modified MDPs, $\langle \mathcal{S}, \mathcal{A}^\infty, P, R, \tau, \mu_0 \rangle$, where \mathcal{A}^∞ is the set of continuous action sequences, (informally, $\mathcal{A}^\infty \equiv \mathcal{P}(\{\mathbf{a}_{t:t+\Delta t} : \forall t, \Delta t > 0\})$ where $\mathcal{P}(x)$ is the power set of x), and $\tau > 0$ a time-constant. In this system, the reward becomes

$$R(\mathbf{s}_t, \mathbf{a}_{t:t+d}) = \int_t^{t+d} e^{-\tau(\kappa-t)} r(\mathbf{s}_\kappa, \mathbf{a}_\kappa) d\kappa, \quad (7)$$

the transition becomes $P(\mathbf{s}_{t+d}|\mathbf{s}_t, \mathbf{a}_{t:t+d})$ where $\mathbf{s}_{t+d} = \mathbf{s}_t + \int_t^{t+d} \dot{\mathbf{s}}_x dx$, and the discount factor becomes variable, i.e.,

$$\gamma(d) = e^{-\tau d}. \quad (8)$$

By choosing a set of discretization points $t_1 < t_2 < t_3, \dots$, the objective function from 6 can be rewritten as follow:

$$J_\pi^\tau(\theta) = \mathbb{E}_\pi \left[\sum_{i=0}^{\infty} \left(\prod_{j=0}^i \gamma(d_j) \right) R(\mathbf{s}_{t_i}, \mathbf{a}_{t_i:t_{i+1}}) \right] \quad (9)$$

where $d_i = t_{i+1} - t_i$. Notice that Equation 9 is equivalent to Equation 6. This discretization is well known, e.g., [18]. It is interesting to notice that MDPs with variable discounting have been introduced in [19] where the author aims to provide a unified framework for RL. However, in White's work, the variable discount factor is treated as part of the environment, and its effect is studied only on the value estimation. In this work, as we will see, the discount factor is, in practice, decided by the high-level policy (which is devoted to choosing low-policy durations). We also study its effect on the policy gradient update rule.

III. METHOD

Our framework, Continuous-Time Continuous-Options (CTCO), comprises a policy π , and a set of options encoded as a parametric model $\Omega(\omega)$. The policy π selects options with variable durations and decides which option to execute only after the termination of the current option, allowing in this way, the system to determine the decision frequency dynamically. However, different option durations can determine the same effect on the environment (e.g., an option that outputs action $\mathbf{a} = 1$ for 3 seconds is equivalent to three options that output action $\mathbf{a} = 1$ for one second each). Since longer durations are preferable for the learner in case of ambiguity (it requires less number of *decisions*), we introduced a regularization factor that favors longer durations. We implemented the update rule of our framework by taking inspiration from soft actor-critic (SAC) algorithm, a state-of-the-art policy gradient method that includes entropy regularization to achieve efficient exploration [20].

A. The Options

In Section II, we saw that continuous time (time-independent) dynamical systems can be seen as particular MDPs where actions are replaced with continuous sequences of actions (i.e, $\mathbf{a}_{t:t+d}$), and the discount factor becomes variable. However, it is impossible to represent continuous

sequences with a finite memory. One way to mitigate this issue is to parameterize these sequences as

$$\{\mathbf{a}_t = \Omega(\mathbf{s}_t, \omega, t, d) : t \in [0, d]\}, \quad (10)$$

where the option Ω can be implemented with any formula, neural network, or program that depends on a vector of parameters ω , the current state \mathbf{s}_t , time t , and duration variable d . Motivated to obtain a simple model with few parameters that can be computed fast (which is ideal for real-time computations), we encoded options using a linear parametric model without state dependency

$$\{\mathbf{a}_t = \Omega(\omega, t, d) = \phi^\top(t/d)\omega : t \in [0, d]\}. \quad (11)$$

Inspired by work on movement primitives, we opt to encode the features ϕ with normalized radial basis functions (RBFs), ensuring that the sequence of actions is *smooth* and produce movements that contain low jerkiness and are ideal for robotic applications. The number of RBFs determines the complexity of the movement. With one RBF, we obtain a constant action output (similar to ARRL), while with more RBFs, we obtain a more complicated output. We designed options without the dependency from the state \mathbf{s}_t opting for open-loop controllers. However, the policy π , compensates for the lack of feedback since it selects options by observing the current state of the environment \mathbf{s}_t .

B. The Policy

The policy π is responsible for choosing the parameters ω and the duration d of the options. In particular, the policy receives as input the current state of the systems \mathbf{s} and determines the probability density of the parameter vector and the duration independently, i.e.,

$$\omega, d \sim \pi_\theta(\cdot, \cdot | \mathbf{s}). \quad (12)$$

The probability density function of ω is modeled as a multidimensional Gaussian distribution while the density function of d is a transformation of Gaussian distribution to positive numbers by applying an invertible function; we choose the sigmoid function. We parameterize the policy using a neural network that outputs $\mu_\theta^\omega(\mathbf{s}_t)$, $\sigma_\theta^\omega(\mathbf{s}_t)$, $\mu_\theta^d(\mathbf{s}_t)$, $\sigma_\theta^d(\mathbf{s}_t)$ as mean and variance of the Gaussian distributions to sample the parameters vector ω and the duration d given observation of state \mathbf{s}_t . To sample ω and d , and compute the gradients of the objective (eq. 9) w.r.t. the policy parameters we use the reparametrization trick,

$$\omega = \mathbf{f}_\theta^\omega(\mathbf{s}; \epsilon) := \mu_\theta^\omega(\mathbf{s}) + \epsilon \sigma_\theta^\omega(\mathbf{s}) \quad (13)$$

$$d = \mathbf{f}_\theta^d(\mathbf{s}; \epsilon) := \text{Sigm}(\mu_\theta^d(\mathbf{s}) + \epsilon \sigma_\theta^d(\mathbf{s})), \quad (14)$$

with $\epsilon, \epsilon \sim \mathcal{N}(\mathbf{0}, \mathbf{I})$. In what follows the evaluation and improvement of the parameterized policy is described.

C. A Soft Actor-Critic Framework

From the perspective of the discretized MDP introduced in Section II, (ω, d) represent the continuous sequence of actions $\mathbf{a}_{t:t+d}$, therefore, can be considered as the action in the discretized MDP. Taking into account this consideration,

Algorithm 1 Continuous-Time Continuous-Option

Require: a policy π with a set of parameters θ, θ' , critic parameters χ, χ' , option model Ω , learning-rates λ_q, λ_p , replay buffer \mathcal{B}
 $i = 0, t_i = 0$, observe s_0
while True **do**
 $\omega_i, d_i \sim \pi_\theta(s_{t_i})$ \triangleright sample option and duration
 Execute $\Omega(\omega_i, \kappa, d_i)$ for $\kappa = 0$ to d_i seconds
 $i \leftarrow i + 1$
 $t_i = t_{i-1} + d_{i-1}$
 Observe s_{t_i} and compute R_{i-1} with (15)
 Store $s_{t_{i-1}}, \omega_{i-1}, d_{i-1}, R_{i-1}, s_{t_i}$ in \mathcal{B}
 Sample s, ω, d, R, s' from \mathcal{B}
 $\chi \leftarrow \chi - \lambda_q \nabla_\chi J\mathcal{L}_Q(\chi, s, \omega, d, R, s')$ \triangleright critic update
 $\theta \leftarrow \theta - \lambda_p \nabla_\theta \mathcal{L}_\pi(\theta, s, \omega, d)$ \triangleright actor update
 Perform soft-update of χ' and θ'
end while

the reward definition in Section II and the option definition in (11), we obtain the reward that depends on state, option parameters, and option duration,

$$R(s_t, \omega, d) = \int_t^{t+d} e^{-\tau(\kappa-t)} r(s_\kappa, \Omega(\omega, \kappa, d)) d\kappa. \quad (15)$$

Notice that $R(s, \omega, d)$ cannot, in general, be computed in closed-form, but it can be approximated via numerical integration. In this MDP, the overall objective becomes

$$J_\pi^\tau(\theta) = \mathbb{E}_\pi \left[\left(\prod_{i=0}^{\infty} \gamma(d_i) \right) R_i \right].$$

where $R_i = R(s_{t_i}, \omega_i, d_i)$, $t_i = \sum_{j=0}^i d_j$, d_i are option durations chosen by the policy π , and s_{t_i} are the observed states.

Until now, we have described a mathematical framework that describes how a policy π_θ interacts with a continuous environment, but we have not defined how such policy can be improved. Among many different options, we choose to implement our algorithm following the soft actor-critic (SAC) architecture [20]. To this end, we include an entropic regularization term that encourages the exploration of different option parameters ω and durations d . Furthermore, we include a new component that penalizes short options. This additional regularizer, called *high-frequency penalization* is needed, since the learner can find solution that works well with arbitrarily high frequency, but such high frequency is detrimental for training performances [21]. The high-frequency penalization consists in a constant term that is subtracted from the objective each time the policy performs a decision. The overall objective incorporates both the entropic and the frequency regularization terms,

$$J_\pi^\tau(\theta) = \mathbb{E}_\pi \left[\sum_{i=0}^{\infty} (R_i + \beta_E \mathcal{H}(\pi(\cdot | s_{t_i})) - \beta_h) \prod_{j=0}^i \gamma(d_j) \right] \quad (16)$$

where β_E and β_h are respectively the entropic regularizer and the high-frequency penalization term. In addition to this regularization terms, following the SAC architecture, we introduce an approximator for the Q -function \hat{Q}_χ , a target Q -function $\hat{Q}_{\chi'}$ and a target policy $\pi_{\theta'}$.

Policy Evaluation. The Q -function evaluates the policy at any state-action pair. In CTCO, the Q -function is described by the following Bellman equation,

$$Q^\pi(s, \omega, d) = \mathbb{E}_{\omega', d', s'} \left[R(s, \omega, d) - \beta_E \log \pi(\omega, d | s) - \beta_h + \gamma(d) Q^\pi(s', \omega', d') \right] \quad (17)$$

where $\omega', d' \sim \pi_{\theta'}(s')$ and $\pi_{\theta'}$ is the target policy. In practice, such equation cannot be solved in closed form. A popular approximate solution consist in introducing two function approximators \hat{Q}_χ and $\hat{Q}_{\chi'}$ that represent the Q -function and the target Q -function respectively. Similarly to SAC, our algorithm minimizes the mean square error

$$\mathcal{L}_Q(\chi, s, \omega, d, s') = \left(\hat{Q}_\chi(s, \omega, d) - R(s, \omega, d) + \beta_E \log \pi(\omega, d | s) + \beta_h - \gamma(d) \hat{Q}_{\chi'}(s', \omega', d') \right)^2 \quad (18)$$

and use a soft-update rule to update χ and χ' (i.e., $\chi' = (1 - \alpha_\chi) \chi' + \alpha_\chi \chi$).

Policy improvement. The classic policy gradient theorem does not take in account situations where the policy changes the action duration and the discount factor. We derived, therefore, the policy gradient taking into account of this new assumption,

$$\begin{aligned} \nabla_\theta J_\pi^\tau(\theta) &= \nabla_\theta \mathbb{E}_\pi \left[(R_i + \beta_E \mathcal{H}(\pi(\cdot | s_{t_i})) - \beta_h) \prod_{i=0}^{\infty} \gamma(d_i) \right] \\ &\propto \mathbb{E}_{\mu_\pi^\rho} \left[\nabla_\omega Q^\pi(s, \omega, d) \nabla_\theta f_\theta^\omega(s, \epsilon) + \nabla_d Q^\pi(s, \omega, d) \nabla_\theta f_\theta^d(s, \epsilon) \right. \\ &\quad \left. - \beta_E \nabla_\theta \log \pi(\omega, d | s) \right]_{\omega=f_\theta^\omega(s, \epsilon), d=f_\theta^d(s, \epsilon)}. \end{aligned} \quad (19)$$

The proof of policy gradient derivation can be found in VII-A. Hence, one can minimize the following surrogate objective

$$\begin{aligned} \mathcal{L}(\theta, s, \omega, d) &= \nabla_\omega Q^\pi(s, \omega, d) \Big|_{\omega=f_\theta^\omega(s, \epsilon)} f_\theta^\omega(s, \epsilon) \\ &\quad + \nabla_d Q^\pi(s, \omega, d) \Big|_{d=f_\theta^d(s, \epsilon)} f_\theta^d(s, \epsilon) \\ &\quad - \beta_E \nabla_\theta \log \pi(\omega, d | s) \end{aligned} \quad (20)$$

The policy gradient in Equation 19 allows to estimate the gradient from samples, as in classic actor-critic frameworks. A scheme of CTCO is presented in Algorithm 1.

IV. EMPIRICAL ANALYSIS

In this section, we focus on answering two questions:

- 1) Is our algorithm robust w.r.t. high interaction frequency with the environment?
- 2) How does our algorithm perform on a real-robotic task?

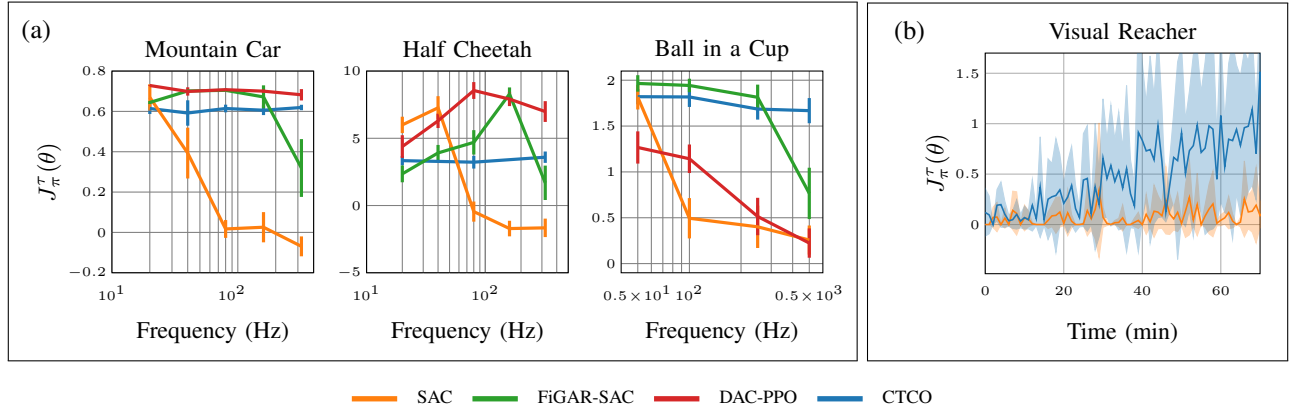


Fig. 2: (a) **Frequency analysis plots.** CTCO’s performance is not damped by high interaction frequency with the environment. (b) **Visual reacher performance.** CTCO reaches higher performances w.r.t. SAC. Bars and shaded areas depicts 95% confidence intervals.

Comparisons. We compare our algorithm against classic RL by using soft actor-critic (SAC), ARRL by using fine-grained action repetition (FiGAR-SAC) [10], and HRL by using double actor-critic (DAC-PPO) [8]. The algorithms are modified to simulate an asynchronous interaction with the environment.

Experimental Setup. When interacting with the real world, the amount of computation that a learning algorithm performs is independent of the task execution. While in the simulation we can perform a fixed number of updates between two different `step()` calls on the simulator, in real-world, action signals and algorithm updates are asynchronous [22]. In this section, we study how different interaction frequencies impact the algorithms. To emulate a realistic effect of different interaction frequencies we modified accordingly the simulated environments, and we modified the algorithms to keep a fixed number of updates per time unit. Furthermore, the discount factor of the discrete-time baselines (SAC, FiGAR-SAC and DAC-PPO) needs to be revised to keep a consistent performance metric across different frequencies. This scaling is obtained by setting $\gamma = \exp(-\tau dt)$ where $\tau = -\log \gamma_{\text{base}}/dt_{\text{base}}$ and $\gamma_{\text{base}} = 0.98$ is the chosen discount factor for a fixed time interval $dt_{\text{base}} = 0.05s$. The algorithms are implemented using PyTorch and NumPy. The structure of the actor is kept identical across the different baselines, except for the last layer that needs to be adapted to the correct output size for our algorithm. In detail, the actor neural network has 2 hidden layers of 10 neurons. The critic neural network, instead, has two hidden layers of 64 neurons. For CTCO we use high frequency penalty $\beta_h = 0.01$ and options with $n_{RBF} = 2$ for all tasks. The implementations are publicly available ¹.

A. Robustness to interaction frequencies

In classic RL, interaction and decision frequencies are the same. Due to this design choice, high interaction fre-

quencies negatively impact performance. In this experiment, we test SAC, FiGAR-SAC, DAC-PPO and our algorithm for different interaction frequencies on three different environments: Mountain Car, Half Cheetah and Ball in a Cup from OpenAI Gym, and MuJoCo [23], [24]. We hypothesize that in continuous control, RL frameworks which choose an action for each task time-step are not robust to high-frequency interactions. One issue arises in terms of exploration that is when the action-cycle time becomes small, the change in the state vanishes and the agent cannot explore the task state-space efficiently, given that the behavior of the actor in the first stages of learning is independently random in each time-step. To examine this hypothesis, we setup the tasks of Mountain Car and Ball in a Cup with sparse rewards, and Half Cheetah with dense rewards for different action-cycle times and measure discounted returns. For each algorithm, we run 30 seeds for 400 minutes of task time. Fig. 2a shows that the performance of SAC, FiGAR-SAC and DAC-PPO is influenced by interaction frequency. However, Our algorithm maintains almost constant performance across the range of different frequencies. In Half Cheetah it has sub-optimal performance, suggesting that with dense reward, simpler algorithms like SAC and FiGAR-SAC achieve higher performance.

B. Real-World performance analysis

To test the ability of CTCO to work in a real-world scenario, we designed a sparse reward visual-reaching task. Although target reaching can be efficiently solved by using classic robotic techniques such as visual servoing, object detection, and planning, it is still interesting to analyze how an RL agent performs in such tasks. Learning from visual input in real-world scenarios without any policy pretraining is in fact very challenging. Visual inputs are subject to noisy observations, and learning algorithms need to be highly efficient to manage learning the task in a reasonable time. For this task, we use a 7 DoF Franka-Emika Panda manipulator shown in Fig. 3. We attach a RGB camera to the robot’s wrist. A bean bag is randomly placed on the table, and the

¹<https://github.com/amir-karimi96/continuous-time-continuous-option-policy-gradient>

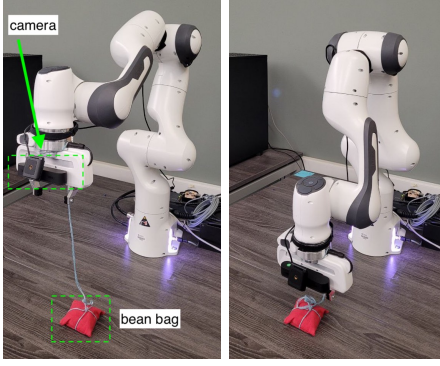


Fig. 3: **Visual Reacher.** **Left:** Before each episode, the robot sets randomly the position of the red bean bag on the table. The goal of the robot is to reach the bean bag by using visual inputs. **Right:** The reward signal is defined zero everywhere, except one when the robot is close enough to the bean bag. The evaluation results are shown in Fig. 2(b).

goal of the robot is to get close enough to the bean bag while it appears in the wrist camera image. The observation consists of a 80×60 RGB image and joint configurations. The agent controls the robot joint velocities (7 dimensions) at 50Hz. Note that the image observation is actually sampled at 25 Hz and upsampled to 50 Hz by repetition. Each episode takes 8s to complete. The sparse reward R is computed as

$$\rho = \sum_{p \in \text{red pixels}} (0.5 - |p_x|)(0.5 - |p_y|) \quad (21)$$

$$\begin{cases} R = 1 & \rho > 0.015 \\ R = 0 & \text{o.w,} \end{cases}$$

where ρ is a dense reward that shows how big and close to the center the bean bag is in the image. $w = 80$, $h = 60$ are image dimensions and $p_x, p_y \in [-0.5, 0.5]$ are normalized coordinates of red pixels in the camera image. The robot has the bean bag attached to its wrist by a string. This allows the robot to set the position of such bean bag randomly on the table at the beginning of each episode. The position of the end-effector is bounded to a box of dimensions $40 \times 60 \times 30 \text{ cm}^3$.

In this experiment, we test SAC against CTCO with $\beta_h = 0.02$, $n_{RBF} = 2$. Both actor and critics, which are identical for the two algorithms except for the actor's last layer, have a convolutional encoder as the first layer followed by fully connected layers. Interactions and agent updates happen in separate processes to allow real-time control, similarly to [22]. Figure 2b shows the average and confidence interval of discounted returns over 5 runs. This result shows that CTCO benefits from the temporal exploration introduced by the continuous options, while SAC fails due to ineffective exploration when the interaction frequency is relatively high. In the video included in supplementary material, we observe how our algorithm exhibits smoother motions both during the initial exploration and training. This smooth exploration is preferable to preserve the robotic articulations in good health.

V. LIMITATIONS

Our proposed algorithm suffers from two significant drawbacks: it introduces two new hyper-parameters and has open-loop options. The two new hyper-parameters define the number of RBFs composing the options and the high-frequency penalization. The performance of the agent can be sensitive to the choice of these hyperparameters for different reward scales and complexity levels of the task. In our work, options are open-loop controllers. Therefore, they cannot adapt to unexpected state changes (stochastic environments). Technically, the policy can counter-react this deficit by choosing low-duration options (thus increasing the frequency of the feedback loop). However, lower duration policies are undesirable, since they complicate learning. This limitation can be compensated by using closed-loop sub-policies, or implementing termination policies as in [18].

VI. CONCLUSION AND FUTURE WORK

Most reinforcement learning algorithms are defined in discrete time. The system is agnostic of what happens between one action and the next. Furthermore, the decision of which action to apply is taken at fixed time intervals. When those intervals are too short, the learning agent needs to make many consecutive decisions before reaching its goal, making the problem harder to solve. In contrast, when decisions are not frequent enough, the system can become uncontrollable. In our paper, we propose a reinforcement learning framework where the agent selects new sub-policies called options with variable durations. In this way, our algorithm becomes robust w.r.t. the underlying interaction frequency and provides high-level, smooth exploration. Empirical results underpin this robustness and show the effectiveness of our algorithm in sparse reward settings and for robotic manipulation. As for future work, we will include a termination mechanism that allows the selection of a new option before the natural termination of the previous one to counteract unforeseen events due to stochasticity in the environment.

REFERENCES

- [1] R. S. Sutton and A. G. Barto, *Reinforcement Learning: An Introduction*. MIT press, 2018.
- [2] S. Kleff, A. Meduri, R. Budhiraja, N. Mansard, and L. Righetti, "High-frequency nonlinear model predictive control of a manipulator," in *2021 IEEE International Conference on Robotics and Automation (ICRA)*. IEEE, 2021, pp. 7330–7336.
- [3] J. Kober and J. Peters, "Learning Motor Primitives for Robotics," in *2009 IEEE International Conference on Robotics and Automation*. IEEE, 2009, pp. 2112–2118.
- [4] M. Dalal, D. Pathak, and R. R. Salakhutdinov, "Accelerating Robotic Reinforcement Learning via Parameterized Action Primitives," *Advances in Neural Information Processing Systems*, vol. 34, 2021.
- [5] K. Mülling, J. Kober, O. Kroemer, and J. Peters, "Learning to select and generalize striking movements in robot table tennis," *The International Journal of Robotics Research*, vol. 32, no. 3, pp. 263–279, 2013.
- [6] D. Surovik, O. Melon, M. Geisert, M. Fallon, and I. Havoutis, "Learning an Expert Skill-Space for Replanning Dynamic Quadruped Locomotion over Obstacles," 2021, publisher: Journal of Machine Learning Research.
- [7] R. S. Sutton, D. Precup, and S. Singh, "Between MDPs and Semi-MDPs: A Framework for Temporal Abstraction in Reinforcement Learning," *Artificial intelligence*, vol. 112, no. 1-2, pp. 181–211, 1999, publisher: Elsevier.

- [8] S. Zhang and S. Whiteson, "Dac: The Double Actor-Critic Architecture for Learning Options," *Advances in Neural Information Processing Systems*, vol. 32, 2019.
- [9] A. Lakshminarayanan, S. Sharma, and B. Ravindran, "Dynamic Action Repetition for Deep Reinforcement Learning," in *Proceedings of the AAAI Conference on Artificial Intelligence*, vol. 31, no. 1, 2017.
- [10] S. Sharma, A. Srinivas, and B. Ravindran, "Learning to repeat: Fine Grained Action Repetition for Deep Reinforcement Learning," *arXiv preprint arXiv:1702.06054*, 2017.
- [11] K. Doya, "Reinforcement learning in continuous time and space," *Neural computation*, vol. 12, no. 1, pp. 219–245, 2000.
- [12] C. Yildiz, M. Heinonen, and H. Lähdesmäki, "Continuous-time model-based reinforcement learning," in *International Conference on Machine Learning*. PMLR, 2021, pp. 12 009–12 018.
- [13] T. Xiao, E. Jang, D. Kalashnikov, S. Levine, J. Ibarz, K. Hausman, and A. Herzog, "Thinking while moving: Deep reinforcement learning with concurrent control," in *International Conference on Learning Representations*, 2019.
- [14] T. P. Lillicrap, J. J. Hunt, A. Pritzel, N. Heess, T. Erez, Y. Tassa, D. Silver, and D. Wierstra, "Continuous Control with Deep Reinforcement Learning," in *International Conference on Learning Representations*, 2016, arXiv: 1509.02971. [Online]. Available: <http://arxiv.org/abs/1509.02971>
- [15] D. Korenkevych, A. R. Mahmood, G. Vasan, and J. Bergstra, "Autoregressive Policies for Continuous Control Deep Reinforcement Learning," *arXiv preprint arXiv:1903.11524*, 2019.
- [16] M. Mutti, R. De Santi, and M. Restelli, "The Importance of Non-Markovianity in Maximum State Entropy Exploration," *arXiv preprint arXiv:2202.03060*, 2022.
- [17] A. R. Mahmood, D. Korenkevych, B. J. Komer, and J. Bergstra, "Setting up a Reinforcement Learning Task with a Real-World Robot," in *2018 IEEE/RSJ International Conference on Intelligent Robots and Systems (IROS)*. IEEE, 2018, pp. 4635–4640.
- [18] S. Park, J. Kim, and G. Kim, "Time Discretization-Invariant Safe Action Repetition for Policy Gradient Methods," *Advances in Neural Information Processing Systems*, vol. 34, pp. 267–279, 2021.
- [19] M. White, "Unifying Task Specification in Reinforcement Learning," in *Proceedings of the 34th International Conference on Machine Learning*. JMLR. org, 2017, pp. 3742–3750.
- [20] T. Haarnoja, A. Zhou, P. Abbeel, and S. Levine, "Soft Actor-Critic: Off-Policy Maximum Entropy Deep Reinforcement Learning with a Stochastic Actor," in *Proceeding of the 35th International Conference on Machine Learning*, 2018, pp. 1856–1865.
- [21] A. Harutyunyan, W. Dabney, D. Borsa, N. Heess, R. Munos, and D. Precup, "The Termination Critic," pp. 2231–2240, 2019.
- [22] Y. Yuan and A. R. Mahmood, "Asynchronous reinforcement learning for real-time control of physical robots," in *2022 International Conference on Robotics and Automation (ICRA)*. IEEE, 2022, pp. 5546–5552.
- [23] G. Brockman, V. Cheung, L. Pettersson, J. Schneider, J. Schulman, J. Tang, and W. Zaremba, "OpenAI Gym," *arXiv:1606.01540*, 2016, arXiv: 1606.01540. [Online]. Available: <http://arxiv.org/abs/1606.01540>
- [24] E. Todorov, T. Erez, and Y. Tassa, "Mujoco: A physics engine for model-based control," in *2012 IEEE/RSJ international conference on intelligent robots and systems*. IEEE, 2012, pp. 5026–5033.

VII. APPENDIX

A. Continuous time policy gradient theorem and proof

Assume parameterizing the policy by θ , According to the bellman equation we have gradient of Q w.r.t to θ as:

$$\begin{aligned}
\nabla_\theta Q(\mathbf{s}, \boldsymbol{\omega}, d) &= \nabla_\theta \mathbb{E}_{\mathbf{s}', \boldsymbol{\omega}', d'} \left[R(\mathbf{s}, \boldsymbol{\omega}, d) - \beta_h + \gamma(d)(Q(\mathbf{s}', \boldsymbol{\omega}', d') + \beta_E \mathcal{H}(\pi_\theta(\cdot, \cdot | \mathbf{s}')))) \right] \\
&= \nabla_\theta \mathbb{E}_{\mathbf{s}', \boldsymbol{\omega}', d'} \left[R(\mathbf{s}, \boldsymbol{\omega}, d) - \beta_h + \gamma(d)(Q(\mathbf{s}', \boldsymbol{\omega}', d') - \beta_E \log(\pi_\theta(\boldsymbol{\omega}', d' | \mathbf{s}')))) \right] \\
&\text{Using reparameterization trick we have} \\
&= \mathbb{E}_{\mathbf{s}', \epsilon'} \left[\gamma(d) (\nabla_{\boldsymbol{\omega}} Q(\mathbf{s}', \boldsymbol{\omega}', d') \nabla_\theta f_\theta^\omega(\mathbf{s}', \epsilon') + \nabla_d Q(\mathbf{s}', \boldsymbol{\omega}', d') \nabla_\theta f_\theta^d(\mathbf{s}', \epsilon')) \right. \\
&\quad \left. + \gamma(d) \nabla_\theta Q(\mathbf{s}', \boldsymbol{\omega}', d') - \gamma(d) \nabla_\theta \beta_E \log(\pi_\theta(\boldsymbol{\omega}', d' | \mathbf{s}')) \right]_{\boldsymbol{\omega}' = f_\theta^\omega(\mathbf{s}', \epsilon'), d' = f_\theta^d(\mathbf{s}', \epsilon')} \\
&\text{We can recursively replace } \nabla_\theta Q(\mathbf{s}', \boldsymbol{\omega}', d') \text{ and obtain} \\
&= \mathbb{E}_{\mu_\pi} \left[\sum_{i=0}^{\infty} \left(\prod_{j=0}^i \gamma(d_j) \right) \left(\nabla_{\boldsymbol{\omega}} Q(\mathbf{s}_{i+1}, \boldsymbol{\omega}_{i+1}, d_{i+1}) \nabla_\theta f_\theta^\omega(\mathbf{s}_{i+1}, \epsilon_{i+1}) + \nabla_d Q(\mathbf{s}_{i+1}, \boldsymbol{\omega}_{i+1}, d_{i+1}) \nabla_\theta f_\theta^d(\mathbf{s}_{i+1}, \epsilon_{i+1}) \right. \right. \\
&\quad \left. \left. - \beta_E \nabla_\theta \log(\pi_\theta(\boldsymbol{\omega}_{i+1}, d_{i+1} | \mathbf{s}_{i+1})) \right) \right]_{\boldsymbol{\omega}_{i+1} = f_\theta^\omega(\mathbf{s}_{i+1}, \epsilon_{i+1}), d_{i+1} = f_\theta^d(\mathbf{s}_{i+1}, \epsilon_{i+1})} \quad \mathbf{s}_0 = \mathbf{s}, \boldsymbol{\omega}_0 = \boldsymbol{\omega}, d_0 = d
\end{aligned} \tag{22}$$

Hence,

Theorem 1 (Continuous-Time Continuous-Option Policy Gradient): Consider a CT-MDP and a sampling process for $\mathbf{s}_i, \boldsymbol{\omega}_i, d_i$ as described in Section III-C. The gradient of the objective w.r.t. to the policy parameter is

$$\begin{aligned}
\nabla_\theta J_\pi &= \mathbb{E}_{\mu_\pi} \left[\sum_{i=0}^{\infty} \left(\prod_{j=0}^{i-1} \gamma(d_j) \right) \left(\nabla_{\boldsymbol{\omega}} Q(\mathbf{s}_i, \boldsymbol{\omega}_i, d_i) \nabla_\theta f_\theta^\omega(\mathbf{s}_i, \epsilon_i) + \nabla_d Q(\mathbf{s}_i, \boldsymbol{\omega}_i, d_i) \nabla_\theta f_\theta^d(\mathbf{s}_i, \epsilon_i) \right. \right. \\
&\quad \left. \left. - \beta_E \nabla_\theta \log(\pi_\theta(\boldsymbol{\omega}_i, d_i | \mathbf{s}_i)) \right) \right]_{\boldsymbol{\omega}_i = f_\theta^\omega(\mathbf{s}_i, \epsilon_i), d_i = f_\theta^d(\mathbf{s}_i, \epsilon_i)}
\end{aligned}$$

where $\gamma(d_i) = e^{-\rho d_i}$ (note that $\prod_{j=0}^{-1} \gamma(d_j) = 1$).

Since the sampling variables $\boldsymbol{\omega}_i, d_i, \dots$ are Markov, we can assume that there is a discounted stationary distribution ζ^ρ from which we can sample them i.i.d. and obtain the same result.

Proof:

$$\begin{aligned}
J_\pi &= \mathbb{E}_{\mu_\pi} \left[\sum_{i=0}^{\infty} \left(\prod_{j=0}^{i-1} \gamma(d_j) \right) (R(\mathbf{s}_i, \boldsymbol{\omega}_i, d_i) - \beta_h + \mathcal{H}(\pi_\theta(\cdot, \cdot | \mathbf{s}_i))) \right] \\
&= \mathbb{E}_{\mathbf{s}_0, \boldsymbol{\omega}_0, d_0} \left[Q(\mathbf{s}_0, \boldsymbol{\omega}_0, d_0) - \log \pi_\theta(\boldsymbol{\omega}_0, d_0 | \mathbf{s}_0) \right] \\
\nabla_\theta J_\pi &= \nabla_\theta \mathbb{E}_{\mathbf{s}_0, \boldsymbol{\omega}_0, d_0} \left[Q(\mathbf{s}_0, \boldsymbol{\omega}_0, d_0) - \log \pi_\theta(\boldsymbol{\omega}_0, d_0 | \mathbf{s}_0) \right]
\end{aligned}$$

By reparameterization trick we have

$$\begin{aligned}
\nabla_\theta J_\pi &= \mathbb{E}_{\mathbf{s}_0, \epsilon_0} \left[\nabla_\theta Q(\mathbf{s}_0, \boldsymbol{\omega}_0, d_0) \right. \\
&\quad + \nabla_{\boldsymbol{\omega}} Q(\mathbf{s}_0, \boldsymbol{\omega}_0, d_0) \nabla_\theta f_\theta^\omega(\mathbf{s}_0, \epsilon_0) + \nabla_d Q(\mathbf{s}_0, \boldsymbol{\omega}_0, d_0) \nabla_\theta f_\theta^d(\mathbf{s}_0, \epsilon_0) \\
&\quad \left. - \beta_E \nabla_\theta \log(\pi_\theta(\boldsymbol{\omega}_0, d_0 | \mathbf{s}_0)) \right]_{\boldsymbol{\omega}_0 = f_\theta^\omega(\mathbf{s}_0, \epsilon_0), d_0 = f_\theta^d(\mathbf{s}_0, \epsilon_0)}
\end{aligned}$$

Replacing $\nabla_\theta Q(\mathbf{s}_0, \boldsymbol{\omega}_0, d_0)$ using equation 22 we have

$$\begin{aligned}
\nabla_\theta J_\pi &= \mathbb{E}_{\mu_\pi} \left[\sum_{i=0}^{\infty} \left(\prod_{j=0}^{i-1} \gamma(d_j) \right) \left(\nabla_{\boldsymbol{\omega}} Q(\mathbf{s}_i, \boldsymbol{\omega}_i, d_i) \nabla_\theta f_\theta^\omega(\mathbf{s}_i, \epsilon_i) + \nabla_d Q(\mathbf{s}_i, \boldsymbol{\omega}_i, d_i) \nabla_\theta f_\theta^d(\mathbf{s}_i, \epsilon_i) \right) \right. \\
&\quad \left. - \beta_E \nabla_\theta \log(\pi_\theta(\boldsymbol{\omega}_i, d_i | \mathbf{s}_i)) \right]_{\boldsymbol{\omega}_i = f_\theta^\omega(\mathbf{s}_i, \epsilon_i), d_i = f_\theta^d(\mathbf{s}_i, \epsilon_i)}
\end{aligned}$$

Discounting can be dropped to stochastically sample from the discounted distribution

$$\begin{aligned}
\nabla_\theta J_\pi &= \mathbb{E}_{\mu_\pi^\rho} \left[\nabla_{\boldsymbol{\omega}} Q(\mathbf{s}, \boldsymbol{\omega}, d) \nabla_\theta f_\theta^\omega(\mathbf{s}, \epsilon) + \nabla_d Q(\mathbf{s}, \boldsymbol{\omega}, d) \nabla_\theta f_\theta^d(\mathbf{s}, \epsilon) \right. \\
&\quad \left. - \beta_E \nabla_\theta \log(\pi_\theta(\boldsymbol{\omega}, d | \mathbf{s})) \right]_{\boldsymbol{\omega} = f_\theta^\omega(\mathbf{s}, \epsilon), d = f_\theta^d(\mathbf{s}, \epsilon)}
\end{aligned}$$